

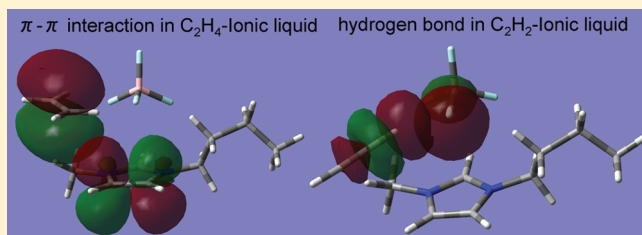
Differential Solubility of Ethylene and Acetylene in Room-Temperature Ionic Liquids: A Theoretical Study

Xu Zhao, Huabin Xing,* Qiwei Yang, Rulong Li, Baogen Su, Zongbi Bao, Yiwen Yang, and Qilong Ren*

Key Laboratory of Biomass Chemical Engineering of Ministry of Education, Department of Chemical and Biological Engineering, Zhejiang University, Hangzhou 310027, China

S Supporting Information

ABSTRACT: The room-temperature ionic liquids (RTILs) have potential in realizing the ethylene (C_2H_4) and acetylene (C_2H_2) separation and avoiding solvent loss and environmental pollution compared with traditional solvents. The interaction mechanisms between gases and RTILs are important for the exploration of new RTILs for gas separation; thus, they were studied by quantum chemical calculation and molecular dynamics simulation in this work. The optimized geometries were obtained for the complexes of C_2H_4/C_2H_2 with anions (Tf_2N^- , BF_4^- , and OAc^-), cation ($bmim^+$), and their ion pairs, and the analysis for geometry, interaction energy, natural bond orbital (NBO), and atoms in molecules (AIM) was performed. The quantum chemical calculation results show that the hydrogen-bonding interaction between the gas molecule and anion is the dominant factor in determining the solubility of C_2H_2 in RTILs. However, the hydrogen-bonding interaction, the $p-\pi$ interaction in C_2H_4 -anion, and the $\pi-\pi$ interaction in C_2H_4 -cation are weak and comparable, which all affect the solubility of C_2H_4 in RTILs with comparable contribution. The calculated results for the distance of $H_{gas}\cdots X$ ($X = O$ or F in anions), the BSSE-corrected interaction energy, the electron density of $H_{gas}\cdots X$ at the bond critical point (ρ_{BCP}), and the relative second-order perturbation stabilization energy ($E(2)$) are consistent with the experimental data that C_2H_2 is more soluble than C_2H_4 in the same RTILs and the solubility of C_2H_4 in RTILs has the following order: $[bmim][Tf_2N] > [bmim][OAc] > [bmim][BF_4]$. The calculated results also agree with the order of C_2H_2 solubility in different RTILs that $[bmim][OAc] > [bmim][BF_4] > [bmim][Tf_2N]$. Furthermore, the calculation results indicate that there is strong C_2H_2 -RTIL interaction, which cannot be negligible compared to the RTIL-RTIL interaction; thus, the regular solution theory is probably not suitable to correlate C_2H_2 solubility in RTILs. The molecular dynamics simulation results show that the hydrogen bond between the H in C2 of the imidazolium cation and the anion will weaken the hydrogen-bonding interaction of the gas molecule and anion in a realistic solution condition, especially in the C_2H_4 -RTIL system.



1. INTRODUCTION

Ethylene and acetylene are very important chemical feedstocks for many products in petrochemical industries such as plastics, lubricants, intermediates, polymers, and so on.^{1–3} Low-temperature distillation, extractive distillation, and physical absorption/adsorption are typical processes for separation of olefins from paraffins^{4,5} that are expensive, especially for feeds with low fractions of olefins, and they consume large amounts of energy. Chemical absorption/adsorption of olefins with metallic ions such as silver and copper ions can be applied promisingly for separating such gaseous mixtures as those ions have no tendency to absorb paraffins.^{6–8} However, it is susceptible to deactivate absorbents or adsorbents by feed contaminants; therefore, chemical absorption/adsorption processes may not be acceptable for applications where tight control of the feed composition is impossible.⁴ On the other hand, the separation and purification for a mixture of ethylene and acetylene also has practical significance. Ethylene, obtained mainly from naphtha or natural gas cracking, usually contains less than 3% mole fraction of acetylene as an impurity due to their close boiling points. Acetylene production through coal

cracking by plasma, a developing technology, also contains a small amount of ethylene (nearly 0.93% mole fraction in a unit of acetylene).⁹ The removal of acetylene from ethylene through a partial hydrogenation of acetylene into ethylene over a noble metal catalyst like supported Pd¹⁰ often results in an overhydrogenation reaction to produce ethane and cause the loss of ethylene. Solvent absorption of acetylene using an organic solvent, such as *N,N*-dimethylformamide (DMF) or *N*-methylpyrrolidinone (NMP),¹¹ has the disadvantages of solvent loss and environmental pollution. Therefore, developing novel capture and separation methods for ethylene and acetylene is desired.

As a kind of green and environmentally friendly solvent, the room-temperature ionic liquids (RTILs) provide a new manner to resolve these problems because of their unique properties, including high thermal stabilities, nearly nonvolatility, and tunable structures and properties.¹² The RTILs are considered

Received: November 17, 2011

Revised: February 23, 2012

Published: March 13, 2012

as possible “green” solvent replacements for many volatile organic solvents. A great deal of effort has focused on the absorption of ethylene and acetylene in RTILs. Camper et al.^{13,14} measured the solubility of ethylene and other gaseous olefins in imidazolium-based and pyridinium-based RTILs. Scovazzo et al. reported the solubility of ethylene and other gaseous hydrocarbons in phosphonium-based¹⁵ and ammonium-based¹⁶ RTILs. The experimental results manifest that olefins have larger solubility compared with paraffins with the same carbon number; thus, RTILs have the potential to be used as a green solvent to separate olefins and paraffins.^{13–16} The solubility of ethylene in RTILs could be correlated with a low deviation using regular solution theory (RST) at low pressures.^{13,14,17,18} The solubility of acetylene and ethylene in various RTILs was measured by Palgunadi and Kim et al.,^{19–21} and acetylene has a much larger solubility than ethylene in RTILs, and a selectivity of acetylene to ethylene up to 43 was achieved using 1,3-dimethylimidazolium methylphosphite ($[\text{dmim}][\text{MeHPO}_3]$) as an absorbent. However, the solubility of acetylene in RTILs could not be correlated with a satisfactory deviation using RST.¹⁹ It was important to find that the solubility of acetylene in RTILs increased with increasing Kamlet-Taft hydrogen-bond basicity (β) of the RTILs.²¹ Quantum mechanical calculations were also performed by Kim et al.,²¹ and the geometry analysis demonstrated that the acidic proton of acetylene specifically formed a hydrogen bond with a basic oxygen atom on the anion of 1-ethyl-3-methylimidazolium bis(trifluoromethylsulfonyl)imide ($[\text{emim}][\text{Tf}_2\text{N}]$), 1-ethyl-3-methylimidazolium methylsulfate ($[\text{emim}][\text{MeSO}_4]$), 1-ethyl-3-methylimidazolium methylphosphite ($[\text{emim}][\text{MeHPO}_3]$), and 1-ethyl-3-methylimidazolium dimethylphosphate ($[\text{emim}][\text{Me}_2\text{PO}_4]$). The calculated distance of $\text{O}_{\text{anion}} \cdots \text{H} - \text{C}_{\text{acetylene}}$ was well in agreement with the solubility of acetylene in those RTILs. Up to now, a lot of solubility data and correlation models of ethylene and acetylene have been reported. However, the interaction mechanisms between ethylene/acetylene and RTILs and the explanation of the differential solubility of ethylene and acetylene in RTILs are not clear, which hinders the exploration of new RTILs for C_2H_4 and C_2H_2 separation seriously. In this paper, we attempt to explain the differential solubility of ethylene and acetylene in RTILs by quantum chemical calculation with the natural bond orbital (NBO) and atoms in molecules (AIM) analysis to better understand the ethylene and acetylene solubilization mechanism. The NBO and AIM analysis can offer us a deeper insight into the interaction mechanism than that of simple geometry analysis. Besides, the calculated results were also used to explain the failure of correlating acetylene solubility in RTILs using the RST. A molecular dynamics simulation was carried to analyze the interaction of the gas and RTILs in a realistic solution condition.

2. METHODS OF CALCULATION

2.1. Ab Initio Calculation of Quantum Chemistry. The geometry optimization was performed on $\text{C}_2\text{H}_4/\text{C}_2\text{H}_2$ -anions, $\text{C}_2\text{H}_4/\text{C}_2\text{H}_2$ -cations, and $\text{C}_2\text{H}_4/\text{C}_2\text{H}_2$ -ion pairs using the Gaussian 03 program.²² Three typical RTILs, 1-butyl-3-methylimidazolium tetrafluoroborate ($[\text{bmim}][\text{BF}_4]$), 1-butyl-3-methylimidazolium bis(trifluoromethylsulfonyl)imide ($[\text{bmim}][\text{Tf}_2\text{N}]$), and 1-butyl-3-methylimidazolium acetate ($[\text{bmim}][\text{OAc}]$), which have low, moderate, and high solubility for $\text{C}_2\text{H}_4/\text{C}_2\text{H}_2$, respectively, were selected as model RTILs. Preliminary geometry optimizations were performed at the

Hartree–Fock (HF) level using the 6-31+G** basis set, starting from various initial configurations without symmetry restrictions. Then, the preliminary optimized geometries were used as input configurations for final optimization at the second-order Moller–Plesset (MP2) level using the 6-31+G** basis set. All optimized configurations were verified as minima without imaginary frequency by full calculation of the Hessian and a harmonic frequency analysis. Interaction energies were corrected for the basis set superposition error (BSSE) by means of the counterpoise correction of Boys and Bernardi.²³ The NBO analysis²⁴ and AIM analysis of the optimized geometries were used to provide a deeper insight into the interactions between the gas and RTILs. The NBO analysis was performed by the NBO 3.1 program as implemented in the Gaussian 03 program package at the MP2/6-31+G** level, and the AIM analysis was performed using the AIMALL software.²⁵ In the NBO analysis, the second-order perturbation stabilization energy $E(2)$ associated with delocalization $i \rightarrow j$ is estimated as $E(2) = \Delta E_{ij} = n_i(F_{ij})^2 / (\varepsilon_j - \varepsilon_i)$, where n_i is the donor orbital occupancy, ε_i and ε_j are the diagonal elements, and F_{ij} is the off-diagonal NBO Fock matrix element.

2.2. Molecular Dynamics Simulation. All molecular dynamics simulations were performed in the constant temperature, constant pressure (NPT) ensemble using the GROMACS simulation package.²⁶ The pressure was maintained at the desired set point by means of a Parrinello–Rahman barostat method²⁷ with a relaxation time of 4.0 ps. The temperature was maintained using a V-rescale thermostat²⁸ with a relaxation time of 1.0 ps. Partial atomic charges were derived from the optimized geometry using the RESP method with the R.E.D.-III.4 package.²⁹ The leap-frog algorithm was used to integrate the equations of motion at the simulated conditions.

The systems were placed in a cubic molecular dynamics box with periodic boundary conditions applied along all directions. The electrostatic forces were treated by the PME method. The cutoff distance was set to 1.2 nm. The van der Waals forces were treated by the cutoff method with a switch region between 1.05 and 1.2 nm. Given the Henry’s law constants of C_2H_4 and C_2H_2 , a mixture of 256 bmim^+ , 256 BF_4^- , and 28 C_2H_2 molecules was simulated at 313 K and 1.7 bar for the $\text{C}_2\text{H}_2 - [\text{bmim}][\text{BF}_4]$ system, a mixture of 256 bmim^+ , 256 BF_4^- , and 14 C_2H_4 molecules was simulated at 313 K and 9.6 bar for the $\text{C}_2\text{H}_4 - \text{bmim}][\text{BF}_4]$ system, and a mixture of 256 bmim^+ , 256 OAc^- , and 14 C_2H_4 molecules was simulated at 313 K and 9.1 bar for the $\text{C}_2\text{H}_4 - [\text{bmim}][\text{OAc}]$ system. The force field parameters for $[\text{bmim}][\text{BF}_4]$ and $[\text{bmim}][\text{OAc}]$ were from Liu et al.’s work³⁰ and amber force field. All of the parameters for C_2H_4 and C_2H_2 used were from the OPLS-AA force field. A complete listing of all relevant force field parameters and partial charges is provided in Table S1 (Supporting Information). The simulation time step was 1 fs for $\text{C}_2\text{H}_4/\text{C}_2\text{H}_2 - [\text{bmim}][\text{BF}_4]$ and 0.5 fs for $\text{C}_2\text{H}_4 - [\text{bmim}][\text{OAc}]$. All of the systems were simulated for 1.5 ns.

3. RESULTS AND DISCUSSION

3.1. $\text{C}_2\text{H}_4/\text{C}_2\text{H}_2$ -Anions. The minimum-energy geometries of $\text{C}_2\text{H}_4/\text{C}_2\text{H}_2$ -anions for $\text{C}_2\text{H}_4 - \text{OAc}^-$, $\text{C}_2\text{H}_2 - \text{OAc}^-$, $\text{C}_2\text{H}_4 - \text{BF}_4^-$, $\text{C}_2\text{H}_2 - \text{BF}_4^-$, $\text{C}_2\text{H}_4 - \text{Tf}_2\text{N}^-$, and $\text{C}_2\text{H}_2 - \text{Tf}_2\text{N}^-$ configurations were calculated; the minimum-energy geometries of the complexes are shown in Figure 1, and the BSSE-corrected interaction energies of the complexes are listed in Table 1. The distances of $\text{H}_{\text{gas}} \cdots \text{X}$ ($\text{X} = \text{O}$ or F in anions) between C_2H_4 and

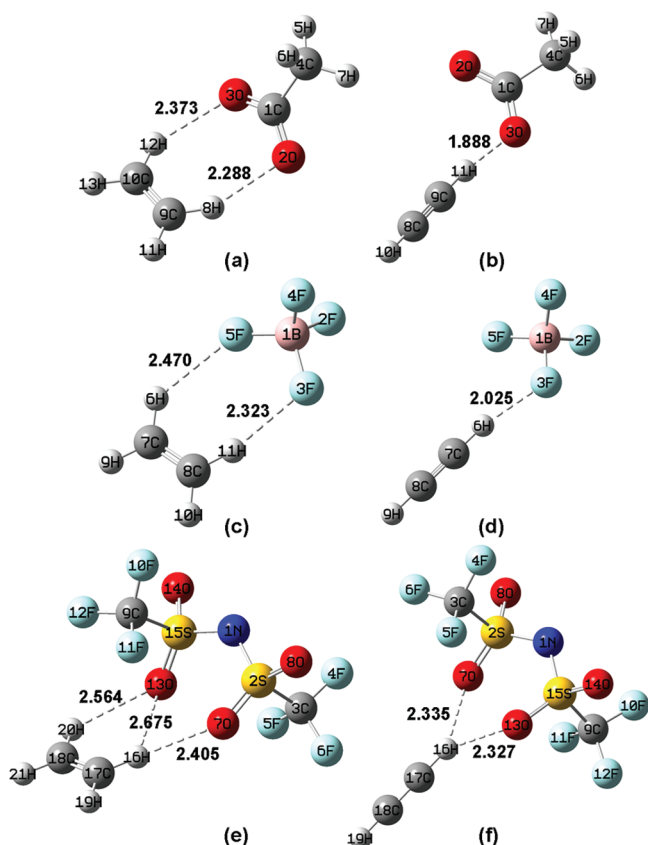


Figure 1. Optimized structures of the complexes of (a) C₂H₄-OAc⁻, (b) C₂H₂-OAc⁻, (c) C₂H₄-BF₄⁻, (d) C₂H₂-BF₄⁻, (e) C₂H₄-Tf₂N⁻, and (f) C₂H₂-Tf₂N⁻. The dotted lines represent the possible modes of interaction, with interatomic distances in angstroms.

Table 1. BSSE-Corrected Interaction Energies (kJ/mol) of the Ions/Ion Pairs with C₂H₄ and C₂H₂

ion and ion pairs	C ₂ H ₄	C ₂ H ₂
BF ₄ ⁻	-13.40	-26.65
OAc ⁻	-22.10	-42.83
Tf ₂ N ⁻	-12.01	-21.36
bmm ⁺	-15.70	-17.80
[bmm][BF ₄]	-12.61	-22.93
[bmm][OAc]	-15.88	-31.52
[bmm][Tf ₂ N]	-23.24	-26.87

the anions range from 2.288 (C₂H₄-OAc⁻) to 2.675 Å (C₂H₄-Tf₂N⁻), whereas the distances of H_{gas}···X between C₂H₂ and the anions are shorter, ranging from 1.888 (C₂H₂-OAc⁻) to 2.335 Å (C₂H₂-Tf₂N⁻). It indicates that hydrogen bonds may occur between C₂H₄/C₂H₂-anions because the distances of H···X are smaller than the sum of van der Waals radii of relevant atoms, as shown in Table 2. Considering that the distances of H_{gas}···X in C₂H₂-anion complexes are shorter than those in C₂H₄-anion complexes with the same anions, the interaction of C₂H₂-anion complexes is stronger than that of

C₂H₄-anion complexes, which is in accordance with the calculated BSSE-corrected interaction energies shown in Table 1. From the data listed in Table 1, we can also find that C₂H₂-OAc⁻ has the highest BSSE-corrected interaction energy of -42.83 kJ/mol, while C₂H₂-Tf₂N⁻ has -21.36 kJ/mol, which is even smaller than that of C₂H₂-BF₄⁻. The same order can also be found in C₂H₄-anion complexes. It can be ascribed to the electron-withdrawing effect of the trifluoromethyl groups, resulting in the reduction of the proton-accepting ability of oxygen. The BSSE-corrected interaction energy and the distance of H_{gas}···X analysis have the same result that the strength of interaction of C₂H₄/C₂H₂-anions is in the order of OAc⁻ > BF₄⁻ > Tf₂N⁻.

To further confirm whether hydrogen bonds exist in the complexes, their topological properties are considered as another criterion. AIM is a technique for studying the paths followed by the electron density between atoms within a molecule. It allows us to study the bonding properties of the systems. According to Bader's topological AIM theory,³² the chemical bonds can be illustrated in terms of the electron density (ρ_{BCP}) and its corresponding Laplacian ($\nabla^2\rho_{BCP}$) at the bond critical point (BCP). The values of ρ_{BCP} and $\nabla^2\rho_{BCP}$ exhibit the characteristics of chemical bonds. The ρ_{BCP} correlates with the strength of an atomic interaction. The sign of $\nabla^2\rho_{BCP}$ is considered to relate to whether the atomic interaction possesses a dominant character of the shared electron (covalent) interactions ($\nabla^2\rho_{BCP} < 0$) or the closed-shell (electrostatic) interactions ($\nabla^2\rho_{BCP} > 0$). The values of ρ_{BCP} and $\nabla^2\rho_{BCP}$ for C₂H₄/C₂H₂-ion complexes are listed in Table 3 and all meet the criterion of the hydrogen bond ($\rho_{BCP} = 0.002\text{--}0.034$ au, $\nabla^2\rho_{BCP} = 0.024\text{--}0.139$ au).³³ Thus, there are really hydrogen bonds in C₂H₄/C₂H₂-anion complexes from the AIM analysis. The values of $\nabla^2\rho_{BCP}$ are all positive, suggesting that the hydrogen-bonding interactions have an electrostatic character. More significantly, the strength of the hydrogen bonds, reflected by the values of ρ_{BCP} , is on the order of C₂H₂-anion > C₂H₄-anion with the same anion, and in C₂H₄/C₂H₂-anion, it is in the order of OAc⁻ > BF₄⁻ > Tf₂N⁻, which is consistent with the BSSE-corrected interaction energy and the length of hydrogen-bond analysis. It should be mentioned that, as opposed to the acidic protons in C₂H₂, the hydrogen bonds in C₂H₄-anion complexes may be in question. Therefore, we tried an infrared spectrum out to further verify whether H-bonding existed in C₂H₄-RTIL. Due to the imidazole-based RTILs having double bonds the as same as C₂H₄, the solubility of C₂H₄ in RTILs is limited, and RTILs always have extremely high responses in infrared analysis; therefore, there was no difference in the infrared spectrum before and after dissolving C₂H₄ in RTILs. However, this style of hydrogen bonding (C-H···X) in C₂H₄-anion complexes is further supported by many previous studies, for example, C-H···R (X = Cl, Br, and I) hydrogen bonds in driving the complexation of nanoscale molecular baskets,³⁴ the C-H···O hydrogen bond in the ethylene-water system,^{35,36} the C-H···N hydrogen bond in the ethylene-ammonia system,³⁷ and the C-H···X (X = C, N, O, F, P, S, and Cl) hydrogen bond of ethylene with first- and second-row hydrides.³⁸

The NBO analysis was performed to give us a further understanding of the orbital interaction of the hydrogen bond and other possible interactions, such as p - π and π - π interactions between C₂H₄/C₂H₂ and ions caused by double bonds or lone pair electrons existing in the ions. The calculated results, listed in Table 4, show the relative second-order

Table 2. van der Waals Radii r_w (Å) of the Elements Involved³¹

	H	C	O	F
r_w	1.20	1.70	1.52	1.47

Table 3. AIM Parameters of Ion/Ion Pairs with C₂H₄ or C₂H₂ and Pure Ion Pairs

species	C ₂ H ₄			C ₂ H ₂		
	H _{gas} ···X	ρ	∇ ² ρ	H _{gas} ···X	ρ	∇ ² ρ
OAc ⁻	H8···O2	0.0144	0.0410	H11···O3	0.0300	0.0828
	H12···O3	0.0122	0.0375			
BF ₄ ⁻	H6···F5	0.0078	0.0344	H6···F3	0.0191	0.0621
	H11···F3	0.0106	0.0407			
Tf ₂ N ⁻	H16···O7	0.0094	0.0329	H16···O7	0.0107	0.0383
	H16···O13	0.0064	0.0259	H16···O13	0.0109	0.0386
	H20···O13	0.0078	0.0295			
[bmim][BF ₄]	H31···F2	0.0059	0.0265	H33···F3	0.0193	0.0641
	H31···F3	0.0056	0.0270			
	H36···F3	0.0081	0.0362			
[bmim][OAc]	H36···O28	0.0139	0.0407	H36···O28	0.0259	0.0749
[bmim][Tf ₂ N]	H44···O33	0.0079	0.0291	H43···O33	0.0089	0.0341
	H44···O38	0.0072	0.0284	H44···O38	0.0101	0.0380
	H46···O38	0.0081	0.0322			
	H _{cation} ···X	ρ	∇ ² ρ	H _{cation} ···X	ρ	∇ ² ρ
[bmim][BF ₄]	H15···F4	0.0130	0.0588	H15···F2	0.0121	0.0559
				H15···F4	0.0125	0.0571
[bmim][OAc]	H7···O26	0.0456	0.1214	H7···O26	0.0450	0.1198
[bmim][Tf ₂ N]	H7···O38	0.0178	0.0596	H7···O38	0.0153	0.0529
	H _{cation} ···X			ρ		∇ ² ρ
pure [bmim][BF ₄]	H15···F2			0.0116		0.0575
	H15···F4			0.0117		0.0580
pure [bmim][OAc]	H7···O26			0.0411		0.1301
pure [bmim][Tf ₂ N]	H7···O38			0.0195		0.0549

perturbation stabilization energy ($E(2)$) between C₂H₄/C₂H₂ and ions. The largest value of $E(2)$ of the strong interaction existing in the C₂H₂–OAc⁻ complex between the lone pair of O3 and σ*(C9–H11) is denoted as LP(O3) → σ*(C9–H11) and is 21.32 kcal/mol. Similarly, the sums of $E(2)$ for LP(X) → σ*(C–H) in C₂H₄–anion complexes are 4.2 (C₂H₄–BF₄⁻), 4.21 (C₂H₄–Tf₂N⁻), and 7.53 kcal/mol (C₂H₄–OAc⁻) and range from 6.22 (C₂H₂–Tf₂N⁻) to 21.32 kcal/mol (C₂H₂–OAc⁻) in C₂H₂–anion complexes. All of the LP(X) → σ*(C–H) interactions indicate the formation of hydrogen bonds between C₂H₄/C₂H₂ and OAc⁻, BF₄⁻, and Tf₂N⁻ anions. The larger the $E(2)$, the stronger the interaction in the orbitals. Thus, the NBO analysis of C₂H₄/C₂H₂–anion agrees with the former analysis that the strength of hydrogen bonds is C₂H₂–anion > C₂H₄–anion with the same anion, and that of C₂H₄/C₂H₂–anion complexes with different anions has the order of OAc⁻ > BF₄⁻ > Tf₂N⁻. (The C₂H₄–BF₄⁻ complex has a larger $E(2)$ of 3.06 than 2.68 kcal/mol in the C₂H₄–Tf₂N⁻ complex, though they have nearly the same sum of $E(2)$.) In C₂H₂–anion complexes, a very weak p –π interaction is found, so that the $E(2)$ for LP(O3) → π*(C8–C9) is 0.19 kcal/mol in the C₂H₂–OAc⁻ complex, the $E(2)$ for LP(F3) → π*(C7–C8) is 0.05 kcal/mol in the C₂H₂–BF₄⁻ complex, and the $E(2)$ values for LP(O7) → π*(C17–C18) and LP(O13) → π*(C7–C8) are 0.16 and 0.15 kcal/mol in the C₂H₂–Tf₂N⁻ complex. There is no p –π interaction in NBO analysis for C₂H₄–anions, maybe because ethylene has only one π bond rather than two as in acetylene.

All of the calculated results shown above validate the existence of hydrogen bonds in C₂H₄/C₂H₂–anion complexes, and they all arrive at the same conclusion that the strength of hydrogen bonds is C₂H₂–anion > C₂H₄–anion with a same anion due to the weakly acidic character of the hydrogen atom in acetylene, and the hydrogen-bonding strength of C₂H₄/

C₂H₂–anion complexes with different anions has the order of OAc⁻ > BF₄⁻ > Tf₂N⁻ caused by the differences in the hydrogen-bond basicity (β) of the RTILs, as shown in Table 5. Notably, the calculated results are in accordance with the experimental solubility data, as shown in Table 5, that the solubility of C₂H₂ is larger than that of C₂H₄ in the same RTILs and the solubility of C₂H₂ in RTILs with different anions has the following order: [bmim][OAc] > [bmim][BF₄] > [bmim][Tf₂N]. It indicates that the hydrogen-bonding interaction may be the dominant factor in determining the solubility of the acetylene in RTILs. However, the calculated results of C₂H₄–anions demonstrate that the solubility of C₂H₄ in RTILs should be [bmim][OAc] > [bmim][BF₄] > [bmim][Tf₂N]. However, the experimental data are in the order of [bmim][Tf₂N] > [bmim][OAc] > [bmim][BF₄]. Thus, there are some other interactions affecting the ethylene solubilization in RTILs besides the weak hydrogen-bonding interaction. On the other hand, the p –π interaction was found in the C₂H₂–anions complex but did not exist in C₂H₄–anions; however, the $E(2)$ was too small to be conclusive.

3.2. C₂H₄/C₂H₂–Cations. After investigating the RTIL's anion–gas interactions, a study on RTIL's cation–gas interaction was performed. The 1-butyl-3-methylimidazolium (bmim⁺) was chosen as the model cation in order to compare with the experimental data. Figure 2 shows the minimum-energy structures of C₂H₄–bmim⁺ and C₂H₂–bmim⁺, and the corresponding energies are tabulated in Table 1. Both the distance of H···C and the BSSE-corrected interaction energy indicate that C₂H₄ and C₂H₂ have a comparable interaction with bmim⁺. The gas molecules are perpendicular to the plane of the imidazolium cation ring, no matter whether the geometry optimization was initiated by (i) aligning the solutes on the same plane of the cation ring and (ii) placing the solutes parallel to but above the plane of the cation ring such that a

Table 4. Involved Donor–Acceptor NBO Interactions and Second-Order Perturbation Stabilization Energies $E(2)$ (kcal/mol) in C_2H_4/C_2H_2 –Ion/Ion Pairs Complexes

donor	acceptor	$E(2)$ (kcal/mol)	donor	acceptor	$E(2)$ (kcal/mol)
$C_2H_4-OAc^-$			$C_2H_2-OAc^-$		
LP(O2)	$\sigma^*(C9-H8)$	5.02	LP(O3)	$\sigma^*(C9-H11)$	21.32
LP(O3)	$\sigma^*(C10-H12)$	2.51	LP(O3)	$\pi^*(C8-C9)$	0.19
$C_2H_4-BF_4^-$			$C_2H_2-BF_4^-$		
LP(F3)	$\sigma^*(C8-H11)$	3.04	LP(F3)	$\sigma^*(C7-H6)$	8.70
LP(F5)	$\sigma^*(C7-H6)$	1.16	LP(F3)	$\pi^*(C7-C8)$	0.05
$C_2H_4-Tf_2N^-$			$C_2H_2-Tf_2N^-$		
LP(O7)	$\sigma^*(C17-H16)$	2.68	LP(O7)	$\sigma^*(C17-H16)$	3.06
LP(O13)	$\sigma^*(C17-H16)$	0.58	LP(O13)	$\sigma^*(C17-H16)$	3.16
LP(O13)	$\sigma^*(C18-H20)$	0.95	LP(O7)	$\pi^*(C17-C18)$	0.16
$C_2H_4-bmim^+$			LP(O13)	$\pi^*(C17-C18)$	0.15
$\pi^*(C3-N4)$	$\pi^*(C27-C28)$	0.10	$C_2H_2-bmim^+$		
$C_2H_4-[bmim][BF_4]$			$\pi^*(C3-N4)$	$\pi^*(C26-C27)$	0.09
LP(F2)	$\sigma^*(C32-H31)$	0.68	$C_2H_2-[bmim][BF_4]$		
LP(F3)	$\sigma^*(C32-H31)$	0.11	LP(F3)	$\sigma^*(C31-H33)$	8.59
LP(F3)	$\sigma^*(C33-H36)$	0.93	$\pi(C6-C7)$	$\pi^*(C31-C32)$	0.21
$\pi(C6-C7)$	$\pi^*(C32-C33)$	0.14	$\pi^*(C6-C7)$	$\pi^*(C31-C32)$	0.11
$\pi^*(C6-C7)$	$\pi^*(C32-C33)$	0.16	$\pi(C31-C32)$	$\pi^*(C6-C7)$	0.41
$\pi(C32-C33)$	$\pi^*(C6-C7)$	0.34	$C_2H_2-[bmim][OAc]$		
$C_2H_4-[bmim][OAc]$			LP(O28)	$\sigma^*(C34-H36)$	15.96
LP(O28)	$\sigma^*(C34-H36)$	1.54			
$\pi(C1-C2)$	$\pi^*(C34-C35)$	0.80			
$\pi(C3-N4)$	$\pi^*(C34-C35)$	0.18			
$\pi^*(C3-N4)$	$\pi^*(C34-C35)$	1.03			
$\pi(C34-C35)$	$\pi^*(C3-N4)$	0.94			
$C_2H_4-[bmim][Tf_2N]$			$C_2H_2-[bmim][Tf_2N]$		
LP(O33)	$\sigma^*(C42-H44)$	1.31	LP(O33)	$\sigma^*(C41-H43)$	1.50
LP(O38)	$\sigma^*(C42-H44)$	0.55	LP(O38)	$\sigma^*(C41-H43)$	1.58
LP(O38)	$\sigma^*(C43-H46)$	0.77	LP(O33)	$\pi^*(C41-C42)$	0.24
LP(O33)	$\pi^*(C42-C43)$	0.06	LP(O38)	$\pi^*(C41-C42)$	0.50
$\pi(C42-C43)$	$\pi^*(C3-N4)$	0.05			

Table 5. Ionic Liquids and Their Absorption Capacities of C_2H_2 and C_2H_4

RTILs	K_H^a of C_2H_4 (bar, 313 K)	ref	K_H of C_2H_2 (bar, 313 K)	ref	β^b	ref
[bmim] [BF ₄]	192.2 ± 3.4	19	16.7 ± 0.3	21	0.376	39
[bmim] [OAc ⁻]	175.9 ± 1.6	19	5.6 ± 0.1	21	1.090	40
[bmim] [Tf ₂ N ⁻]	82.9 ± 1.0	19	21.8 ± 0.1	19	0.243	39

^a K_H is Henry's law constant. ^b β is the Kamlet–Taft parameter of hydrogen-bond basicity.

potential $\pi-\pi$ stacking stabilization could take place. As is well-known, the most positive charge is located on the H7 atom in $bmim^+$ due to the strong inductive effect of the N4 and N8 atoms. Therefore, the weakly electrostatic interaction between H7 and the negatively charged carbon of the gas plays a major role in forming this structure, which is further proved by the consistency with the distance of H···C and the sum of their van der Waals radii in Table 2. In the optimized structures, the gas molecules stabilize on the side of butyl due to the van der Waals force. The NBO analysis, as shown in Table 4, demonstrates that $\pi-\pi$ interaction exists in C_2H_4/C_2H_2 – $bmim^+$ complexes. The $E(2)$ for $\pi^*(C3-N4) \rightarrow \pi^*(C27-C28)$ in C_2H_4 – $bmim^+$ is 0.10 kcal/mol, and that for $\pi^*(C3-N4) \rightarrow \pi^*(C26-C27)$ in C_2H_2 – $bmim^+$ is 0.09 kcal/mol, but

they are weak and much smaller than the hydrogen-bonding interactions in C_2H_4/C_2H_2 –anions complexes.

3.3. C_2H_4/C_2H_2 –Ion Pairs. Finally, the interactions between C_2H_4/C_2H_2 and ion pairs of RTILs were investigated. The optimized structures of the ion pairs and gas–ion pair complexes are shown in Figure 3. On the whole, the solute leans more toward the anion with an orientation almost similar to that of the C_2H_4/C_2H_2 –anion complexes. It indicates that the anions play an important role in determining the C_2H_4/C_2H_2 solubility in RTILs, which is similar to the solubility of other gases in RTILs, such as CO₂.^{41–43} The structures of the RTILs are not perturbed appreciably by the addition of gas molecules.

In C_2H_4/C_2H_2 –[bmim][BF₄] complexes, the gas molecules stabilize on the plane above the imidazolium cations and close to the methyl side due to the steric effects. Unlike minimum-energy structures of C_2H_4/C_2H_2 –[bmim][BF₄] complexes, the gas molecules stabilize on the plane below the imidazolium cations in C_2H_4/C_2H_2 –[bmim][OAc⁻] complexes. One oxygen atom of the acetate has an affinity with the hydrogen atom of the gas solute, and the other one interacts with the hydrogen atom of the imidazolium cation. In C_2H_4/C_2H_2 –[bmim]–[Tf₂N⁻] complexes, the gas molecules are in front of and perpendicular to the plane of the imidazolium cation ring due to the steric effect of [Tf₂N⁻].

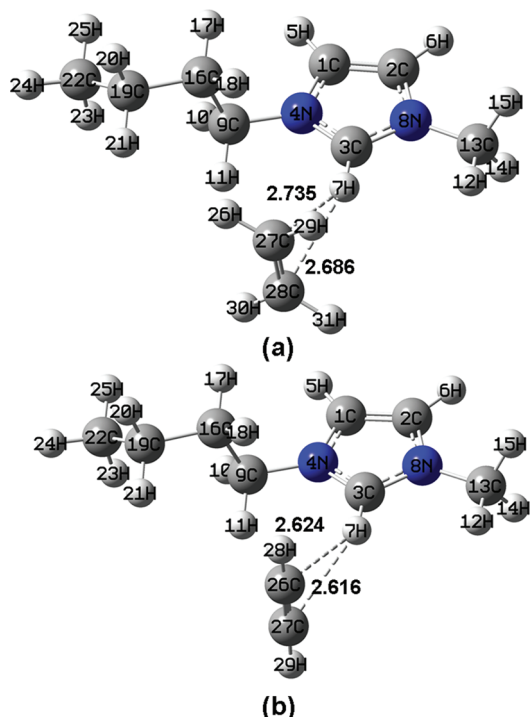


Figure 2. Minimum-energy structures of the complexes of (a) $\text{C}_2\text{H}_4\text{-bmim}^+$, (b) $\text{C}_2\text{H}_2\text{-bmim}^+$. The dotted lines represent the possible modes of interaction, with interatomic distances in angstroms.

The distances of $\text{H}_{\text{gas}}\cdots\text{X}$ ($\text{X} = \text{O}$ or F in anions) between C_2H_4 and the anions in $\text{C}_2\text{H}_4\text{-ion}$ pair complexes range from 2.301 ($\text{C}_2\text{H}_4\text{-[bmim][OAc]}$) to 2.642 Å ($\text{C}_2\text{H}_4\text{-[bmim][Tf}_2\text{N]}$), whereas the distances of $\text{H}\cdots\text{X}$ between C_2H_2 and the anions in $\text{C}_2\text{H}_2\text{-ion}$ pair complexes range from 1.948 ($\text{C}_2\text{H}_2\text{-[bmim][OAc]}$) to 2.455 Å ($\text{C}_2\text{H}_2\text{-[bmim][Tf}_2\text{N]}$). The values of ρ_{BCP} and $\nabla^2\rho_{\text{BCP}}$ in AIM analysis are also on the scale of the hydrogen bond in $\text{C}_2\text{H}_4/\text{C}_2\text{H}_2\text{-ion}$ pair complexes (Table 3). The values of ρ_{BCP} range from 0.0056 ($\text{C}_2\text{H}_4\text{-[bmim][BF}_4]$) to 0.0139 ($\text{C}_2\text{H}_4\text{-[bmim][OAc]}$) in $\text{C}_2\text{H}_4\text{-ion}$ pair complexes and from 0.0089 ($\text{C}_2\text{H}_2\text{-[bmim][Tf}_2\text{N]}$) to 0.0259 ($\text{C}_2\text{H}_2\text{-[bmim][OAc]}$) in $\text{C}_2\text{H}_2\text{-ion}$ pair complexes. The results for the distance and AIM analysis of $\text{C}_2\text{H}_4/\text{C}_2\text{H}_2\text{-ion}$ pairs are similar to those of the $\text{C}_2\text{H}_4/\text{C}_2\text{H}_2\text{-anion}$, which demonstrates that the strength of hydrogen bonds is $\text{C}_2\text{H}_4\text{-ion}$ pairs > $\text{C}_2\text{H}_2\text{-ion}$ pairs with the same ionic liquid, and the hydrogen bonding strength of $\text{C}_2\text{H}_4/\text{C}_2\text{H}_2\text{-ion}$ pair complexes has the order of $[\text{bmim}][\text{OAc}] > [\text{bmim}][\text{BF}_4] > [\text{bmim}][\text{Tf}_2\text{N}]$. From the AIM analysis in Table 3, we can find that the H in C2 of the imidazolium cation forms a hydrogen bond with anion of the type $\text{H}_{\text{cation}}\cdots\text{X}$, and the C_2H_4 forms the hydrogen bond with the anion simultaneously. In other words, in the one-to-one quantum chemical calculation, although the H in C2 of the imidazolium cation competes with the gas molecule to form a hydrogen bond with the anion, the hydrogen bond between the gas molecule and anion can still form, and it will not influence the hydrogen bond between the cation and anion significantly. For example, the value of ρ_{BCP} for $\text{H}7\cdots\text{O}38$ in pure

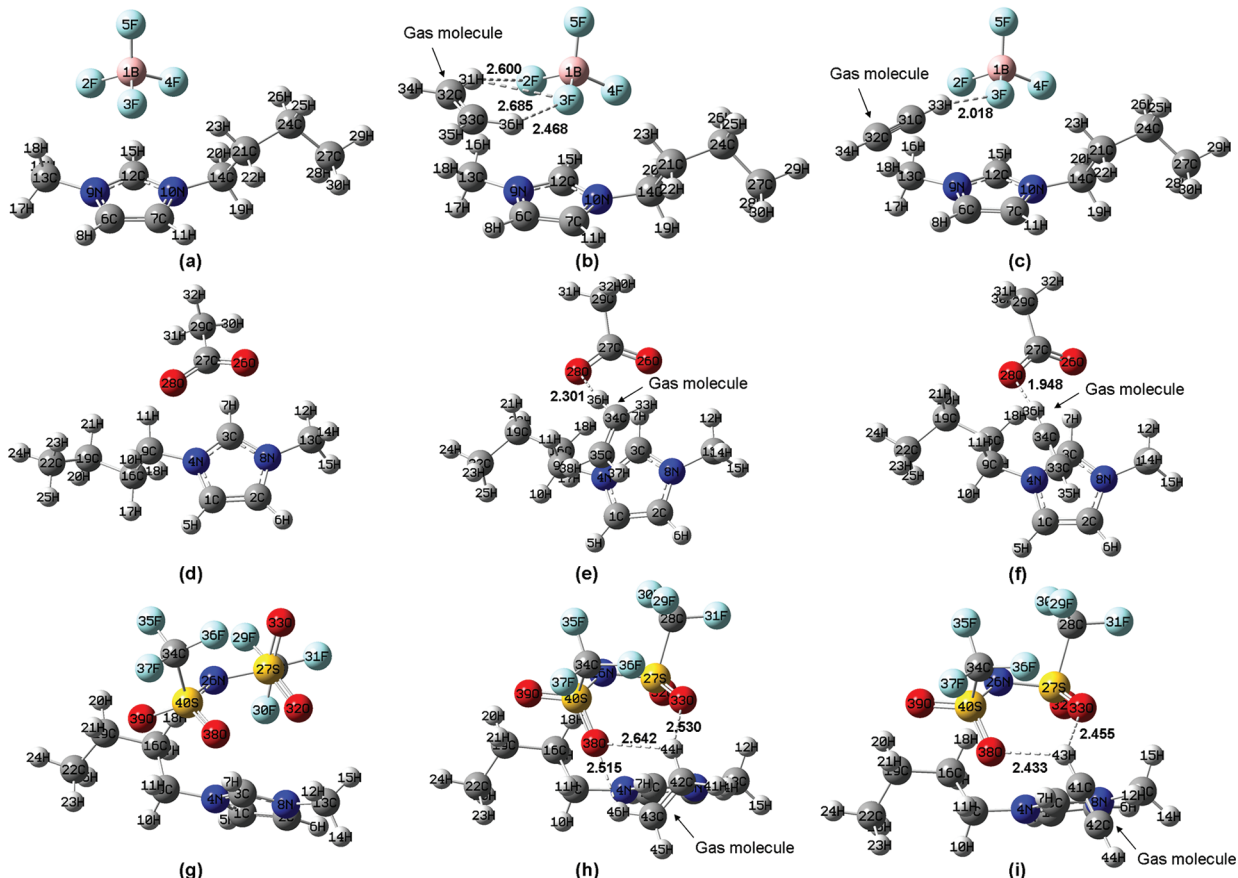


Figure 3. Minimum-energy structures of (a) $[\text{bmim}][\text{BF}_4]$, (b) $\text{C}_2\text{H}_4\text{-[bmim][BF}_4]$, (c) $\text{C}_2\text{H}_2\text{-[bmim][BF}_4]$, (d) $[\text{bmim}][\text{OAc}]$, (e) $\text{C}_2\text{H}_4\text{-[bmim][OAc]}$, (f) $\text{C}_2\text{H}_2\text{-[bmim][OAc]}$, (g) $[\text{bmim}][\text{Tf}_2\text{N}]$, (h) $\text{C}_2\text{H}_4\text{-[bmim][Tf}_2\text{N]}$, and (i) $\text{C}_2\text{H}_2\text{-[bmim][Tf}_2\text{N]}$. The dotted lines represent the possible modes of interaction, with interatomic distances in angstroms.

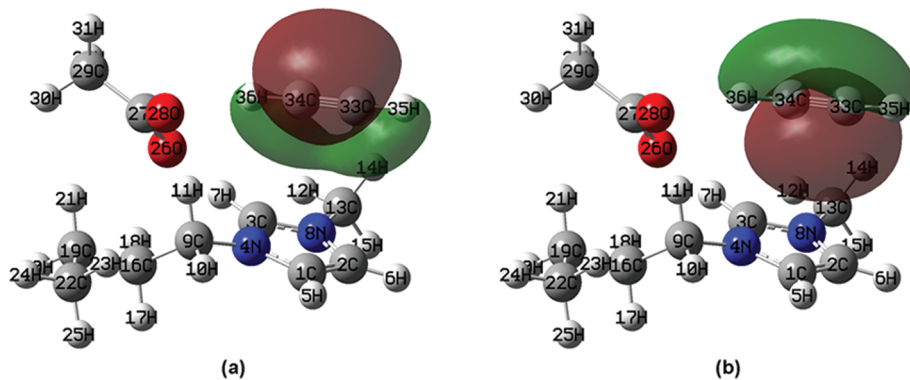


Figure 4. The two unusual natural bond orbitals (a, b) of acetylene in C₂H₂-[bmim][OAc].

[bmim][Tf₂N] is 0.0195, and in C₂H₄-[bmim][Tf₂N] and C₂H₂-[bmim][Tf₂N] complexes, the values are 0.0178 and 0.0153, respectively, within the hydrogen-bonding scale. It seems that the number of H-bond-acceptor sites in the anions influences the final optimized configurations. For [bmim]-[OAc], OAc⁻ has two H-bond-acceptor sites in the O atom; the one bonds to the C2-H of the imidazolium cation, and the other bonds to the gas molecule; therefore, it is apt to form a single C-H...O bond with C₂H₄. However, for [bmim][BF₄] and [bmim][Tf₂N], the two anions have multiple H-bond-acceptor sites; therefore, they are apt to form multiple C-H...O/F bonds.

The relative second-order perturbation stabilization energy $E(2)$ (Table 4) by the NBO analysis can offer us a deeper insight into the interactions between gas solutes and RTILs. The $E(2)$ for $\text{LP(F3)} \rightarrow \sigma^*(\text{C31-H33})$ in the $\text{C}_2\text{H}_2-\text{[bmim][BF}_4]$ complex, representing a hydrogen-bonding interaction, is 8.59 kcal/mol, while the $\pi-\pi$ interaction, the sum of $E(2)$ for $\pi(\text{C6-C7}) \rightarrow \pi^*(\text{C31-C32}), \pi^*(\text{C6-C7}) \rightarrow \pi^*(\text{C31-C32}),$ and $\pi(\text{C31-C32}) \rightarrow \pi^*(\text{C6-C7}),$ is 0.73 kcal/mol. It suggests that the hydrogen-bonding interaction is much stronger than the $\pi-\pi$ interaction in C_2H_2 solubilization in RTILs, and no obvious $p-p$ interaction is found between the gas and anion. Kim has observed a similar phenomenon in $\text{C}_2\text{H}_2-\text{[emim][Tf}_2\text{N}], \text{C}_2\text{H}_2-\text{[emim][MeSO}_4], \text{C}_2\text{H}_2-\text{[emim][MeHPO}_3],$ and $\text{C}_2\text{H}_2-\text{[emim][Me}_2\text{PO}_4]$ systems.²¹ In $\text{C}_2\text{H}_4-\text{[bmim][BF}_4]$, the hydrogen-bonding interaction and $\pi-\pi$ interaction also exist. However, the sums of $E(2)$ for the hydrogen-bonding and $\pi-\pi$ interaction are 1.72 and 0.64 kcal/mol, respectively, indicating that the two interactions are weak and comparable. Thus, both the hydrogen-bonding and $\pi-\pi$ interaction affect the solubility of ethylene in RTILs with comparable contribution.

In $\text{C}_2\text{H}_4/\text{C}_2\text{H}_2$ -[bmim][OAc] complexes, the $E(2)$ for $\text{LP(O28)} \rightarrow \pi^*(\text{C}34-\text{H}36)$, representing the hydrogen-bonding interaction, are 1.54 kcal/mol in C_2H_4 -[bmim][OAc] and 15.96 kcal/mol in C_2H_2 -[bmim][OAc]. This indicates that C_2H_2 can form a stronger hydrogen bond with [bmim][OAc] than C_2H_4 , which is in accordance with the result of the gas-anion calculation. The sum of $E(2)$ for $\pi(\text{C}1-\text{C}2) \rightarrow \pi^*(\text{C}34-\text{C}35)$, $\pi(\text{C}3-\text{N}4) \rightarrow \pi^*(\text{C}34-\text{C}35)$, $\pi^*(\text{C}3-\text{N}4) \rightarrow \pi^*(\text{C}34-\text{C}35)$, and $\pi(\text{C}34-\text{C}35) \rightarrow \pi^*(\text{C}3-\text{N}4)$, the $\pi-\pi$ interactions, is 2.95 kcal/mol in C_2H_4 -[bmim][OAc]. The hydrogen-bonding interaction and $\pi-\pi$ interaction are comparable in C_2H_4 -[bmim][OAc], which also means that both the hydrogen-bonding and $\pi-\pi$ interaction both are main factors in dissolving ethylene in RTILs. The

significance of the $E(2)$ in $\text{C}_2\text{H}_2-\text{[bmim]}\text{[OAc]}$ cannot be figured out. The reason for this is that the natural bond orbitals shown in Figure 4a and b appear simply to be the so-called π “banana bonds” of the acetylene molecule, which are not unusual. Nevertheless, it can be affirmed that the hydrogen-bonding interaction is still much stronger than the $\pi-\pi$ interaction.

In $C_2H_4/C_2H_2-[bmim][Tf_2N]$ complexes, the $[Tf_2N]^-$ has a larger volume compared to $[BF_4]^-$ or $[OAc]^-$ and occupies the plane above the imidazolium cation ring, so that the gas molecule stabilizes in front of the cation and on the plane that is perpendicular to the imidazolium cation ring. Thus, the $\pi-\pi$ interaction weakens due to the steric effect of $[Tf_2N]^-$. The $E(2)$ for $\pi(C42-C43) \rightarrow \pi^*(C3-N4)$ is only 0.05 kcal/mol in $C_2H_4-[bmim][Tf_2N]$, and even no $\pi-\pi$ interaction is found in $C_2H_2-[bmim][Tf_2N]$. However, the $p-\pi$ interaction exists wherein the $E(2)$ for $LP(O33) \rightarrow \pi^*(C42-C43)$ is 0.06 kcal/mol in $C_2H_4-[bmim][Tf_2N]$, and $LP(O33) \rightarrow \pi^*(C41-C42)$ is 0.24 kcal/mol; that for $LP(O38) \rightarrow \pi^*(C41-C42)$ is 0.50 kcal/mol in $C_2H_2-[bmim][Tf_2N]$. Thus, not only the $\pi-\pi$ interaction in C_2H_4 -cation but also the $p-\pi$ interaction in C_2H_4 -anion affects the solubility of C_2H_4 in RTILs with comparable contribution. The sum of $E(2)$ for $LP(O33) \rightarrow \sigma^*(C42-H44)$, $LP(O38) \rightarrow \sigma^*(C42-H44)$, and $LP(O38) \rightarrow \sigma^*(C43-H46)$, representing hydrogen-bonding interactions, is 2.63 kcal/mol in $C_2H_4-[bmim][Tf_2N]$, and for $LP(O33) \rightarrow \sigma^*(C41-H43)$ and $LP(O38) \rightarrow \sigma^*(C41-H43)$, it is 3.08 kcal/mol in $C_2H_2-[bmim][Tf_2N]$. It suggests that the hydrogen-bonding interactions are weak in $C_2H_4/C_2H_2-[bmim][Tf_2N]$. Furthermore, the value of 3.08 kcal/mol is much smaller than 8.59 and 15.96 kcal/mol in $[bmim][BF_4]$ and $[bmim][OAc]$, respectively, which agrees with the experimental solubility data that C_2H_2 solubility has the following order: $[bmim][OAc] > [bmim][BF_4] > [bmim]-[Tf_2N]$.

The BSSE-corrected interaction energy of C_2H_2 -ion pairs is always bigger than that of C_2H_4 -ion pairs (Table 1), which is consistent with the experimental solubility data that C_2H_2 has a higher solubility than C_2H_4 in the same RTIL. In C_2H_4 -ion pair complexes, the calculated results are also in accordance with the experimental data that the C_2H_4 solubility is in the order of $[\text{bmim}][\text{Tf}_2\text{N}] > [\text{bmim}][\text{OAc}] > [\text{bmim}][\text{BF}_4]$. Though the BSSE-corrected interaction energy of C_2H_2 -ion pairs is in the order of $[\text{bmim}][\text{OAc}] > [\text{bmim}][\text{Tf}_2\text{N}] > [\text{bmim}][\text{BF}_4]$, which departs from the experimental data, the distance of $\text{H}_{\text{gas}} \cdots \text{X}$, AIM, and NBO analyses all agree with the solubility data and the β of the RTILs.

In addition, the BSSE-corrected interaction energies of ion pairs were calculated, and the values were -349.78 , -314.94 , and -409.88 kJ/mol for $[\text{bmim}]^+[\text{BF}_4^-]$, $[\text{bmim}]^+[\text{Tf}_2\text{N}^-]$, and $[\text{bmim}]^+[\text{OAc}^-]$, respectively. If we consider the RTIL's ion pair energy as the solvent–solvent interaction energy, the ratio of the gas–ion pair interaction energy (Table 1) to the solvent–solvent interaction energy can be calculated. The C_2H_4 –ion pair interaction ratios are 3.6, 7.4, and 3.9% for $[\text{bmim}]^+[\text{BF}_4^-]$, $[\text{bmim}]^+[\text{Tf}_2\text{N}^-]$, and $[\text{bmim}]^+[\text{OAc}^-]$, respectively. However, the C_2H_2 –ion pair interaction ratios are 6.6, 8.5, and 7.7% for $[\text{bmim}]^+[\text{BF}_4^-]$, $[\text{bmim}]^+[\text{Tf}_2\text{N}^-]$, and $[\text{bmim}]^+[\text{OAc}^-]$, respectively, which are almost twice those in C_2H_4 –ion pair complexes with the same RTIL except $[\text{bmim}]^+[\text{Tf}_2\text{N}^-]$. The studies based on RST assume that the solute–solvent (gas–RTIL) interaction should be negligibly small compared to the solvent–solvent (RTIL–RTIL) and solute–solute interaction.¹³ Given these data, it suggests that the RST is suitable to correlate the C_2H_4 solubility data in RTILs. However, due to the strong solute–solvent interaction between C_2H_2 and RTILs, which is not negligibly small compared to the solvent–solvent interaction, the RST correlation performance for C_2H_2 solubility would be poor. It could be the explanation for the failure of correlating C_2H_2 solubility in RTILs with the solubility parameter based on RST.¹⁹

3.4. Molecular Dynamics Simulation. All of the quantum chemical calculations conducted above are one-to-one and in an ideal gaseous state. It is more interesting and reasonable to study ethylene and acetylene dissolving in RTILs in a more realistic solution condition to discuss the probability of the hydrogen-bonding interaction in solution in the presence of cation competition. Molecular dynamics simulation is an available method that has been used to study the interaction of small-molecule solvents in RTILs.^{42–44} It is quite acceptable that the anion associates with the hydrogen (H6) attached to the C2 carbon on the bmim^+ and forms a hydrogen-bonding interaction^{45–48} due to the relatively large positive charge of the hydrogen.^{39,48} Figure 5a shows the radial distribution functions for the F atom of the BF_4^- about the H6 atom of the imidazolium ring in bmim^+ and the H atom of C_2H_2 , while Figure 5b is the same plot for the F atom of the BF_4^- about the H6 and H atom of C_2H_4 , and Figure 5c is the plot for the O atom of the OAc^- about the H6 and H atom of C_2H_4 . There is very little difference between the $\text{H}_6^{\text{cation}}\text{--F}$ curves in Figure 5a and b, in which a sharp, intense peak is observed at about 2.4 Å; the second peak is lower at about 4.2 Å, which indicates that the strong hydrogen-bonding interaction exists between bmim^+ and BF_4^- . The $\text{H}_{\text{acetylene}}\text{--F}$ curve in Figure 5a has a sharp, intense peak at 2.4 Å, indicating a strong hydrogen-bonding interaction between the H of C_2H_2 and the F of BF_4^- . As in the $\text{H}_{\text{ethylene}}\text{--F}$ curve shown in Figure 5b, the peak between 2.5 and 3.25 Å is low in intensity and broad, which indicates that a very weak interaction exists between C_2H_4 and BF_4^- . Similarly, in Figure 5c, the $\text{H}_6^{\text{cation}}\text{--O}$ curve has a sharp, intense peak at 2.3 Å, and the initial peak of the $\text{H}_{\text{ethylene}}\text{--O}$ curve between 2.5 and 3.25 Å is broad and low in intensity. Compared to the one-to-one quantum chemical calculation, the distance of $\text{H}_{\text{gas}}\cdots\text{X}$ ($\text{X} = \text{O}$ or F in anions) calculated from molecular dynamics simulation is always the larger one. It demonstrates that the hydrogen bond between the H in C2 of the imidazolium cation and the anion will weaken the hydrogen-bonding interaction of the gas molecule and anion, especially in the C_2H_4 –RTIL system.

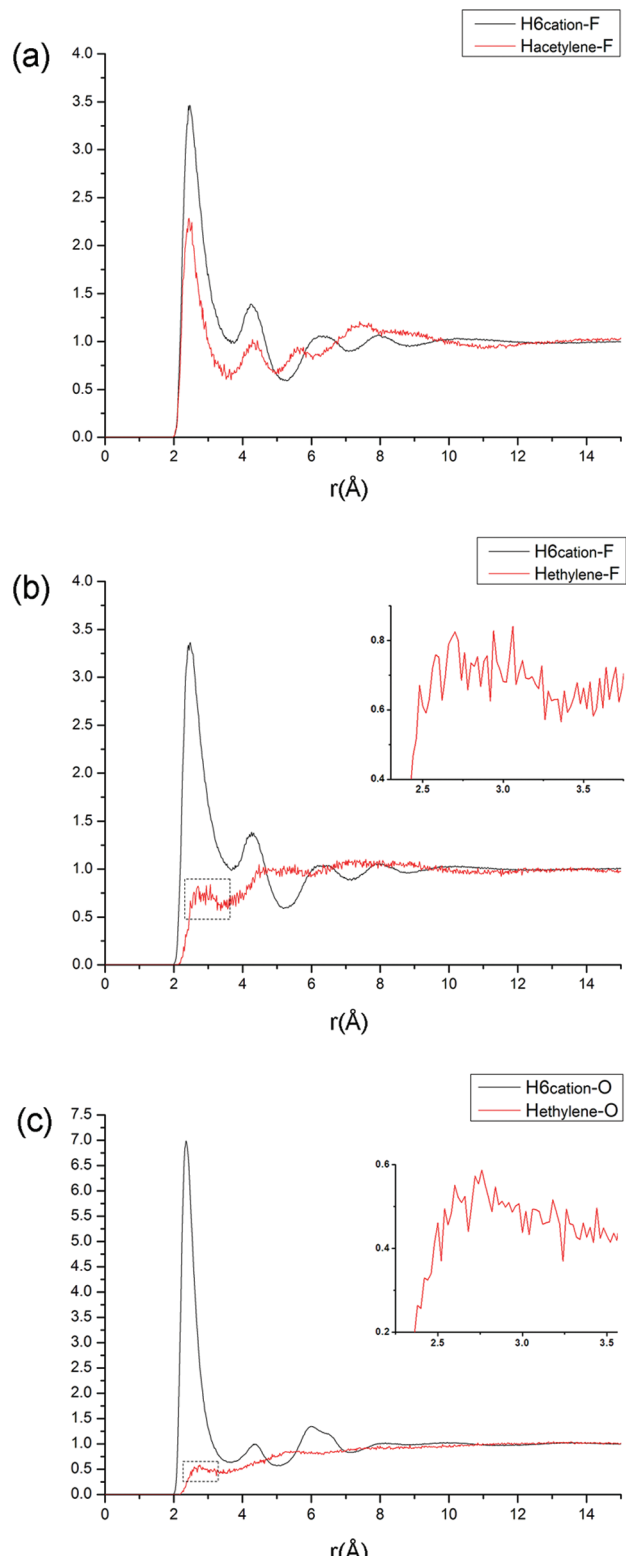


Figure 5. (a) Radial distribution functions for the F atom of the BF_4^- about the H6 atom of the cation (black line) and the H atom of C_2H_2 (red line). (b) The same plots and symbol meaning for C_2H_4 . (c) Radial distribution functions for the O atom of the OAc^- about the H6 atom of the cation (black line) and the H atom of C_2H_4 (red line).

4. CONCLUSION

The minimum-energy geometries of $\text{C}_2\text{H}_4/\text{C}_2\text{H}_2$ –anions, $\text{C}_2\text{H}_4/\text{C}_2\text{H}_2$ –cations, and $\text{C}_2\text{H}_4/\text{C}_2\text{H}_2$ –ion pairs were calcu-

lated, and the geometry analysis, interaction energies analysis, AIM analysis, and NBO analysis were performed. The calculated results show that there are stronger hydrogen bonds between C_2H_2 and RTIL's anions. Furthermore, the hydrogen-bonding interaction between the gas molecule and anion is the dominant factor in determining the solubility of C_2H_2 in RTILs. However, the hydrogen-bonding, $p-\pi$ interaction in C_2H_4 -anions, and $\pi-\pi$ interaction in C_2H_4 -cations are weak and comparable, which all affect the solubility of C_2H_4 in RTILs with comparable contribution.

The calculated results for the distance of $H_{\text{gas}} \cdots X$, BSSE-corrected interaction energy, electron density (ρ_{BCP}) of $H_{\text{gas}} \cdots X$ in AIM analysis, and the relative second-order perturbation stabilization energy ($E(2)$) in NBO analysis are consistent with the previous experimental data that C_2H_2 is more soluble than C_2H_4 in the same RTIL, and the solubility of C_2H_4 in RTILs has the following order: $[\text{bmim}][\text{Tf}_2\text{N}] > [\text{bmim}][\text{OAc}] > [\text{bmim}][\text{BF}_4]$. Though the BSSE-corrected interaction energies of C_2H_2 -ion pairs have some difference from the solubility data, the distance of $H_{\text{gas}} \cdots X$ calculation, ρ_{BCP} of $H_{\text{gas}} \cdots X$ in AIM analysis, and $E(2)$ in NBO analysis are in accordance with the solubility data of C_2H_2 , that is, $[\text{bmim}][\text{OAc}] > [\text{bmim}][\text{BF}_4] > [\text{bmim}][\text{Tf}_2\text{N}]$. Furthermore, the simulation results indicate that there is strong solute–solvent interaction between C_2H_2 and RTILs, which is not negligibly small compared to the solvent–solvent interaction; thus, the RST is probably not suitable to correlate the C_2H_2 solubility in RTILs.

The molecular dynamics simulation results show that the hydrogen bond between the H in C2 of the imidazolium cation and the anion will weaken the hydrogen-bonding interaction of the gas molecule and anion in a realistic solution condition, especially in the C_2H_4 -RTIL system.

ASSOCIATED CONTENT

Supporting Information

A complete listing of all relevant force field parameters and partial charges. This material is available free of charge via the Internet at <http://pubs.acs.org>.

AUTHOR INFORMATION

Corresponding Author

*Telephone and Fax: +86 571 87952375. E-mail: xinghb@zju.edu.cn (H.X.); renql@zju.edu.cn (Q.R.).

Notes

The authors declare no competing financial interest.

ACKNOWLEDGMENTS

The authors are grateful for financial support from the National Natural Science Foundation of China (20936005, 21076175 and 20806066) and Zhejiang Provincial Natural Science Foundation of China (No. Y4080167).

REFERENCES

- (1) Huang, W.; McCormick, J. R.; Lobo, R. F.; Chen, J. G. *J. Catal.* **2007**, *246*, 40–51.
- (2) Yashima, E.; Matsushima, T.; Okamoto, Y. *J. Am. Chem. Soc.* **1997**, *119*, 6345–6359.
- (3) Silvestri, F.; Marrocchi, A. *Int. J. Mol. Sci.* **2010**, *11*, 1471–1508.
- (4) Eldridge, R. B. *Ind. Eng. Chem. Res.* **1993**, *32*, 2208–2212.
- (5) Nymeyer, K.; Visser, T.; Assen, R.; Wessling, M. *J. Membr. Sci.* **2004**, *232*, 107–114.
- (6) Cho, I. H.; Cho, D. L.; Yasuda, H. K.; Marrero, T. R. *J. Chem. Eng. Data* **1995**, *40*, 102–106.
- (7) Duan, S.; Ito, A.; Ohkawa, A. *J. Membr. Sci.* **2003**, *215*, 53–60.
- (8) Won, J.; Kim, D. B.; Kang, Y. S.; Choi, D. K.; Kim, H. S.; Kim, C. K.; Kim, C. K. *J. Membr. Sci.* **2005**, *260*, 37–44.
- (9) Bond, R. L.; Galbraith, I. F.; Ladner, W. R.; McConnell, G. I. T. *Nature* **1963**, *200*, 1313–1314.
- (10) Ruta, M.; Laurenczy, G.; Dyson, P. J.; Kiwi-Minsker, L. *J. Phys. Chem. C* **2008**, *112*, 17814–17819.
- (11) Weissermel, K.; Arpe, H. *Industrial Organic Chemistry*, 4th ed.; Wiley-VCH: Weinheim, Germany, 2003.
- (12) Brennecke, J. F.; Maginn, E. J. *AIChE J.* **2001**, *47*, 2384–2389.
- (13) Camper, D.; Scovazzo, P.; Koval, C.; Noble, R. *Ind. Eng. Chem. Res.* **2004**, *43*, 3049–3054.
- (14) Camper, D.; Becker, C.; Koval, C.; Noble, R. *Ind. Eng. Chem. Res.* **2005**, *44*, 1928–1933.
- (15) Ferguson, L.; Scovazzo, P. *Ind. Eng. Chem. Res.* **2007**, *46*, 1369–1374.
- (16) Condemarin, R.; Scovazzo, P. *Chem. Eng. J.* **2009**, *147*, 51–57.
- (17) Kilaru, P. K.; Condemarin, R. A.; Scovazzo, P. *Ind. Eng. Chem. Res.* **2008**, *47*, 900–909.
- (18) Kilaru, P. K.; Scovazzo, P. *Ind. Eng. Chem. Res.* **2008**, *47*, 910–919.
- (19) Palgunadi, J.; Kim, H. S.; Lee, J. M.; Jung, S. *Chem. Eng. Process.* **2010**, *49*, 192–198.
- (20) Lee, J. M.; Palgunadi, J.; Kim, J. H.; Jung, S.; Choi, Y.; Cheong, M.; Kim, H. S. *Phys. Chem. Chem. Phys.* **2010**, *12*, 1812–1816.
- (21) Palgunadi, J.; Hong, S. Y.; Lee, J. K.; Lee, H.; Lee, S. D.; Cheong, M.; Kim, H. S. *J. Phys. Chem. B* **2011**, *115*, 1067–1074.
- (22) Frisch, M. J.; Trucks, G. W.; Schlegel, H. B.; Scuseria, G. E.; Robb, M. A.; Cheeseman, J. R.; Montgomery, J. A.; Vreven, T.; Kudin, K. N.; Burant, J. C.; et al. *Gaussian 03*, revision E.01; Gaussian, Inc.: Pittsburgh, PA, 2003.
- (23) Boys, S.; Bernardi, F. *Mol. Phys.* **1970**, *19*, 553–566.
- (24) Reed, A. E.; Curtiss, L. A.; Weinhold, F. *Chem. Rev.* **1988**, *88*, 899–926.
- (25) Todd, A.; Keith, T. G. *AIMAll*, version 11.06.19; TK Gristmill Software: Overland Park KS, 2011.
- (26) Hess, B.; Kutzner, C.; van der Spoel, D.; Lindahl, E. *J. Chem. Theory Comput.* **2008**, *4*, 435–447.
- (27) Parrinello, M.; Rahman, A. *J. Appl. Phys.* **1981**, *52*, 7182–7190.
- (28) Bussi, G.; Donado, D.; Parrinello, M. *J. Chem. Phys.* **2007**, *126*, 014101.
- (29) Dupradeau, F.-Y.; Pigache, A.; Zaffran, T.; Savineau, C.; Lelong, R.; Grivel, N.; Lelong, D.; Rosanski, W.; Cieplak, P. *Phys. Chem. Chem. Phys.* **2010**, *12*, 7821–7839.
- (30) Liu, Z.; Huang, S.; Wang, W. *J. Phys. Chem. B* **2004**, *108*, 12978–12989.
- (31) Bondi, A. *J. Phys. Chem.* **1964**, *68*, 441–451.
- (32) Bader, R. F. W. *Chem. Rev.* **1991**, *91*, 893–928.
- (33) Koch, U.; Popelier, P. L. A. *J. Phys. Chem.* **1995**, *99*, 9747–9754.
- (34) Gibb, C. L. D.; Stevens, E. D.; Gibb, B. C. *J. Am. Chem. Soc.* **2001**, *123*, 5849–5850.
- (35) Scheiner, S.; Grabowski, S. J.; Kar, T. *J. Phys. Chem. A* **2001**, *105*, 10607–10612.
- (36) Udagawa, T.; Ishimoto, T.; Tokiwa, H.; Tachikawa, M.; Nagashima, U. *J. Phys. Chem. A* **2006**, *110*, 7279–7285.
- (37) Wetmore, S. D.; Schofield, R.; Smith, D. M.; Radom, L. *J. Phys. Chem. A* **2001**, *105*, 8718–8726.
- (38) Hartmann, M.; Wetmore, S. D.; Radom, L. *J. Phys. Chem. A* **2001**, *105*, 4470–4479.
- (39) Crowhurst, L.; Mawdsley, P. R.; Perez-Arlanidis, J. M.; Salter, P. A.; Welton, T. *Phys. Chem. Chem. Phys.* **2003**, *5*, 2790–2794.
- (40) Ohno, H.; Fukaya, Y. *Chem. Lett.* **2009**, *38*, 2–7.
- (41) Blanchard, L. A.; Gu, Z.; Brennecke, J. F. *J. Phys. Chem. B* **2001**, *105*, 2437–2444.
- (42) Cadena, C.; Anthony, J. L.; Shah, J. K.; Morrow, T. I.; Brennecke, J. F.; Maginn, E. J. *J. Am. Chem. Soc.* **2004**, *126*, 5300–5308.
- (43) Anthony, J. L.; Anderson, J. L.; Maginn, E. J.; Brennecke, J. F. *J. Phys. Chem. B* **2005**, *109*, 6366–6374.

- (44) Hanke, C. G.; Johansson, A.; Harper, J. B.; Lynden-Bell, R. M. *Chem. Phys. Lett.* **2003**, *374*, 85–90.
- (45) Hardacre, C.; McMath, S. E. J.; Nieuwenhuyzen, M.; Bowron, D. T.; Soper, A. K. *J. Phys.: Condens. Matter* **2003**, *15*, S159–S166.
- (46) Meng, Z.; Dolle, A.; Carper, W. R. *THEOCHEM* **2002**, *585*, 119–128.
- (47) Hanke, C. G.; Price, S. L.; Lynden-Bell, R. M. *Mol. Phys.* **2001**, *99*, 801–809.
- (48) Morrow, T. I.; Maginn, E. J. *J. Phys. Chem. B* **2002**, *106*, 12807–12813.